2026 IEEE/SICE International Symposium on System Integration (SII)
January 11-14, 2026. Cancún, México

Calibration of Optical Center Alignment between a High-speed Camera and Galvanometer Mirrors for High-precision Laser Tracking

Tomohiro Sueishi[1], Keiko Yokoyama[2], and Masatoshi Ishikawa[1]

***Abstract*— Controlling laser beam to be directed toward a tracking target with high accuracy is necessary in free-space optical communications and laser processing. If an optical center of a high-speed camera for tracking and a rotational center of a laser scanning system are aligned, three-dimensional calibration becomes unnecessary and wide-area laser tracking projection becomes easier, but it is difficult to precisely align their optical centers only manually. In this paper, we propose an interactive calibration method to precisely align the optical centers using a circular projection on screens with slits on one side, placed in different positions. Image processing visualizes the displacement of the circular parameters on each screen and enables highly accurate alignment in the translational direction. Evaluation experiments have demonstrated sub-pixel accuracy of calibration and fast and accurate laser tracking projection.**

I. Introduction

Techniques that keep a laser beam focused on a predetermined position on an object in motion are in demand for a variety of applications, including free-space optical (FSO) communication [1], [2], laser processing [3], [4], and laser fabrication [5]. When communicating with drones and satellites using laser beams in FSO, it is necessary to irradiate laser beams accurately and without delay to moving targets while dealing with atmospheric fluctuations. In laser processing and fabrication, it is desirable to control the laser beam along an accurate trajectory using feedback control by a sensor system, even on a predetermined trajectory.

Spatial calibration between a camera to track unknown motion and a laser scanning system is necessary when controlling the direction of the laser beam using rotational mirrors towards the motion target. Although there is a three-dimensional calibration method for laser galvanometers and a range camera placed at different locations [6], the spatial range in which positional accuracy can be guaranteed tends to be narrow with the three-dimensional placement and its calibration. A calibration method to align optical centers of a camera and projector has also been proposed [7], since placing the camera and projector at the same optical center by means of a beam splitter enables a wide range of light projection control with only two-dimensional recognition and control. Systems that optically align the camera optical axis with the laser optical axis [4], [5], [8] and tracking projection systems that align the optical axes of the camera and laser scanning system [9] have been proposed, but to the best of the our knowledge, no technique that precisely aligns the optical centers of the camera and laser scanning system has been reported.

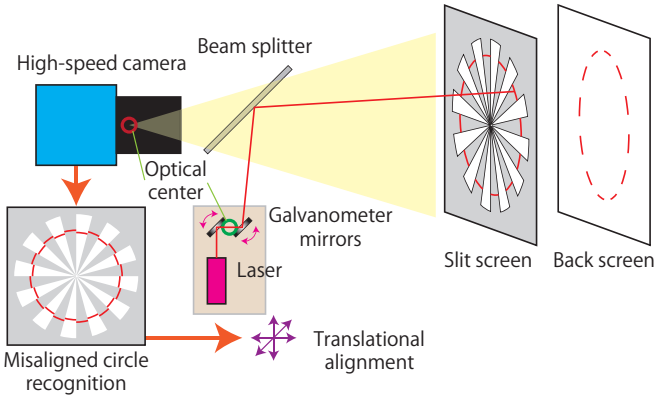

Fig. 1. A concept of the proposed calibration method.

Therefore, in this paper, we propose an interactive calibration method that precisely aligns the optical center of a high-speed camera with the center of rotation of galvanometer mirrors for high-precision laser tracking projection onto a widely moving object through two-dimensional recognition and high-speed visual feedback, whose concept is shown in Fig. 1. In a configuration in which the optical centers of the camera and laser galvanometer mirrors are roughly aligned using a beam splitter, a background screen and a screen with a slit are placed at different depths, and a circular laser trajectory is projected by sinusoidal input to each of the galvanometer mirrors. Appropriate image processing estimates a center position and radius of the circles projected on each screen, and visualizes the optical center misalignment as the misalignment of the center and radius of each circle. The user fine-tunes the position of the laser scanning system (or camera) in the direction of decreasing the circle misalignment to achieve a calibration that precisely aligns the optical centers.

II. Related Works

Free-space optical (FSO) communication establishes communication with moving objects such as trains and satellites through laser control. FSO requires acquisition, tracking, and pointing (ATP) mechanisms such as atmospheric turbulence correction for long-distance communications [1]. In the ATP mechanism, gimbals and fast steering mirrors (FSM) are used as the scanning system, and cameras [10] and quadrant photo detectors (QPD) are used as the sensor system. Optical

[1]T. Sueishi and M. Ishikawa are with Research Institute for Science and Technology, Tokyo University of Science, Niijuku 6-3-1, Katsushika-ku, Tokyo 125-8585, Japan. sueishi@ishikawa-vision.org
[2]K. Yokoyama is with Visual Intelligence Research Laboratories, NEC, 1753 Shimonumabe, Nakahara-ku, Kawasaki-shi, Kanagawa, 211-8666, Japan. k.yokoyama@nec.com

control is applied to beacon lights and reflectors [2] to achieve laser tracking.

In laser processing and fablication, a system in which the camera and laser have the same optical axis has been proposed. Levichev et al. propose a monitoring system during laser cutting in sheet metal processing, in which a fiber laser and a high-speed camera are installed on the same optical axis [4]. Yeung et al. propose an in-situ calibration method for laser powder bed fusion by optical marker recognition using a camera coaxially aligned with the laser [5]. Mikawa et al. propose a figure drawing system using a high-speed camera and an ultraviolet laser with the same optical axis and marker embedding using photochromism [8]. However, in these systems, the laser optical axis is fixed with respect to the camera angle of view [4], [5], [8]. Oku et al. propose a system for drawing figures on moving objects in which the optical axes of a high-speed camera and a laser galvanometer mirror are aligned [9], but there is no mention of optical center alignment.

Liu et al. propose a calibration method for the position and orientation of a single-point laser rangefinder relative to a camera for depth measurement [11]. Sels et al. propose a three-dimensional calibration method with a laser galvanometric scanner including a laser Doppler vibrometer, using a range camera for depth measurement [6]. However, in these methods, neither the optical center nor the optical axis of the camera and the laser system are coincident [6], [11].

Sueishi et al. have realized dynamic projection mapping in which the optical axes of a high-speed camera and a low-frame-rate projector are aligned in a high-speed optical-axis control system using galvanometer mirrors [12] and there is almost no projection misalignment to a moving object only in two-dimensional recognition [13]. On the other hand, there is no mention of precise alignment of the projector and the camera. Yamamoto et al. propose a system in which the pixels of the projector and camera are perfectly aligned using relay optics. The correspondence between the camera and projector pixels is estimated by a homography matrix, but this is not a discussion of optic-center alignment since they share the same objective lens [14].

Calibration methods are also proposed for the coaxial projector camera system. Amano et al. propose an interactive calibration method to precisely align the optical center of the projector-camera by visualizing projection misalignment [7]. The method uses a background screen and a diagonal slit screen at different depth positions, and the vertical and horizontal line grid projection. Huang et al. have also estimated the relative position and orientation of the projector-camera system with high accuracy by calculating the absolute phase using a marker plate and horizontal sinusoidal fringe pattern projection [15]. However, these methods relate to projectors, not laser scanning systems.

III. Proposed Calibration Method

A. System Configuration

The system configuration of the proposed calibration method is shown in Fig. 2. The optical centers of the camera and the laser scanning system are nearly aligned using a beam splitter. Screens are placed at different depths in the laser projection direction. The screen in the foreground has a slit. A function generator signal generates a specific pattern projection of the laser scanning system. A high-speed camera connected to the computer processes the image to identify misalignment in the projected pattern on the screens. Based on the misalignment, we move a stage equipped with the laser scanning system to achieve precise alignment of the optical center.

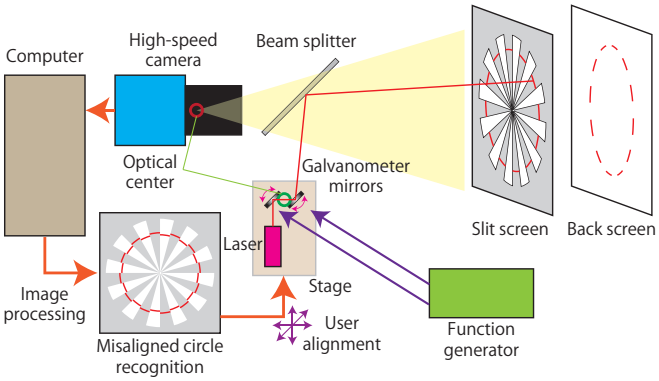

Fig. 2. System configuration of the proposed calibration method.

In this paper, we adopt a galvanometer mirror for the laser scanning system. Although MEMS mirrors have been developed that enable dual-axis rotation with a single mirror [16], we select the galvanometer mirror consisting of two rotating mirrors that can respond quickly, have a wide scanning angle range, and are widely used and readily available. If the projection distance is far enough, the centers of rotation are assumed to be coincident, and the coincident center of rotation is considered to be the optical center of the galvanometer mirror.

B. Design of Projection Pattern

We describe a design policy of the laser projection pattern used for calibration. Unlike the projector [7], the laser scanning system relies on mirror angle control for spatial pattern generation and can project only one point at the same time. Complex pattern projections (e.g., grid points) during the camera exposure time require proper synchronization of mirror angle control and laser source flicker control [17], [18]. Laser drawing of figures with one cycle too long is not suitable for interactive calibration. On the other hand, a figure drawn by a periodic mirror command signal with a continuously emitting laser can be easily used. In particular, it is desirable for the figure to have three or more parameters for the three translational degrees of freedom that can be changed for the optical center alignment.

Although rectangles are easy to use with straight edges and corners as feature points in image processing, they require constant beam brightness and appropriate response to corner overshoot [18], and the frequency response of the laser scanning system used must be adjusted.

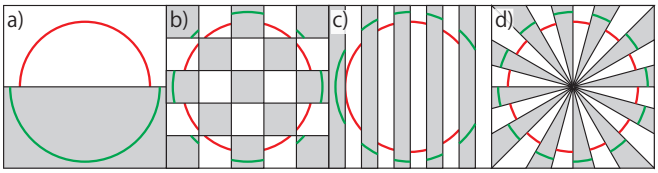

Fig. 3. Design of slit screen with circle projection mislignment. a) half, b) checker, c) stripe, and d) radial.

A circle is a simple closed curve that can be generated by inputting a sinusoidal wave to each of the XY mirrors. Since it is often used in image processing, such as ellipse fitting [19], the circle is used as the projection pattern in this paper. Another reason is that it is easy to obtain the same circle shape even if the amplitude of the sinusoidal wave attenuates due to the inertia of the rotating mirror.

C. Design of Slit Screen

This section describes the design of a slit screen to visualize the misalignment of the optical center. Candidate slits are shown in Fig. 3. Alignment of the optical center requires that the projected circles, divided into two screens, coincide. Note that if the feature points of the ellipse are biased, the ellipse fitting results are also likely to be biased [20]. In addition, due to the distortion of the camera lens and the projection distortion caused by the galvanometer mirror [21], the bias of the feature points of the circle is undesirable. In fact, a half slit in Fig. 3a) produces a large bias in the feature points. A checker pattern in Fig. 3b) and a stripe pattern in Fig. 3c) can be expected to provide some scattering of feature points, but it is difficult to guarantee an even distribution.

Therefore, in this paper, we adopt a radial slit shown in Fig. 3d). The slit is symmetrical with respect to the center of the circle, and even if the center is slightly off-center, a feature point can be expected at each fixed angle. Even if the circle projection is not accurate due to lens distortion or projection distortion [21], feature points with similar distributions are expected to avoid bias in the estimated circle parameters.

The two screens should be of different colors to facilitate the image processing described later. Screens with slits can be easily fabricated by 3D printing.

D. Calibration Procedure

The calibration procedure using the circular projection pattern and the radial slit screen is as follows;

1) input sinusoidal signals of the function generator to the galvanometer mirrors and project the circular pattern onto the back screen,
2) place the slit screen so that the centers of the projected circle and the radial slit are approximately aligned,
3) coarsely adjust the beam splitters and galvanometer mirror positions so that the projected circles on each screen in the camera image approximately match,
4) estimate projection circle parameters and their difference on each screen by image processing (Sec. III-E),
5) adjust the stage with galvanometer mirrors so that the circular parameter difference approaches zero and the optical centers of the camera and galvanometer mirror are aligned, and
6) map the XY coordinates of the image to the angles of the galvanometer mirror using a two-dimensional projection (e.g., grid points) onto the back screen.

Basically, as with the projector calibration method [7], it is a coarse-to-fine alignment using a slit screen, but the projection pattern and error visualization methods are significantly different.

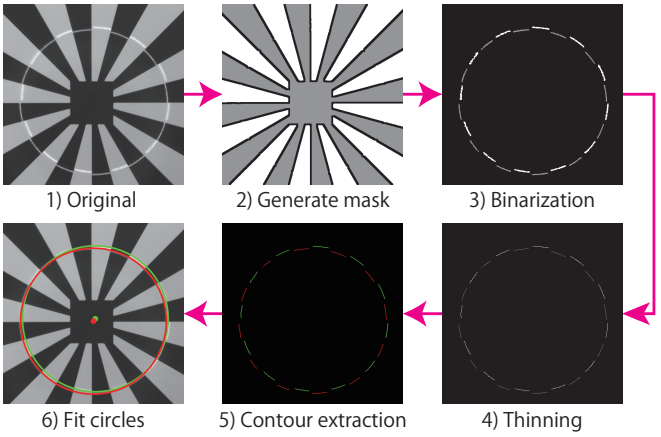

Fig. 4. Detection image processing of the projected circle divided by the slit.

E. Circle Detection Image Processing

The circle detection image processing (Fig. 4) to visualize the optical center misalignment is as follows; 1) take images of laser projection, the slit and back screen with sufficient contrast, 2) generate mask areas showing each screen by binarization at specific threshold values and applying erosion, and dilation, 3) extract the laser projection area by adaptive binarization in the mask areas, 4) apply a thinning process [22], [23], 5) extract feature points of the projected circles by contour extraction, and 6) perform circle fitting [19].

In 2) generating the mask areas, the laser region is assumed to be sufficiently narrower than the radial slit, so that the laser region is eliminated by the erosion and dilation process. In addition, the mask areas are slightly eroded to avoid the influence of noisy feature points near the slit contour. 3) Adaptive binarization within the mask area is binarization by a threshold value that is a constant added to the average luminance value within a rectangular region around each pixel (and also corresponding to the mask area). This excludes the influence of bias in the luminance distribution on the screen. 4) The thinning process [22] is to exclude the effect of thickness due to laser and camera blur. In particular, for interactive procedure, this paper uses an implementation intended for high-speed processing [23]. For 6) circle fitting, we set appropriate initial values of the circle center (x_c, y_c) and radius r for the feature points $\boldsymbol{x}_i = (x_i, y_i)$. The following equation is then solved by the least-

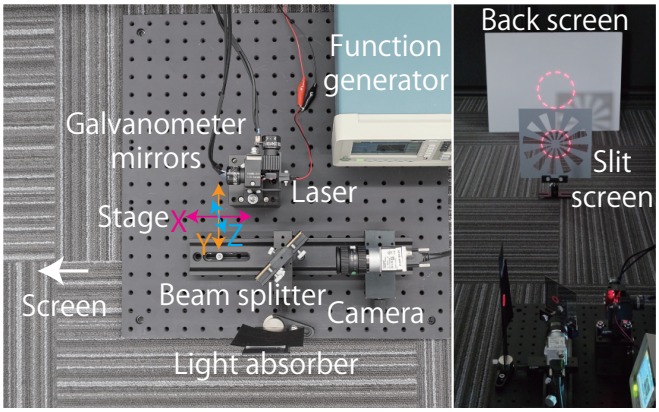

Fig. 5. Experimental system.

squares method using the Levenberg-Marquard algorithm [19],

$$\arg\min_{x_c,y_c,r} \sum_i \left(\sqrt{(x_i - x_c)^2 + (y_i - y_c)^2} - r \right)^2 . \quad (1)$$

IV. Experimental Evaluation

A. Experimental System

An evaluation experiment system is shown in Fig. 5. The high-speed camera was a Basler acA800-510um (monochrome, 800×600 px, exposure 40,000 μs, approx. 25 fps) with a 25 mm focal length lens. The galvanometer mirror was a Thorlabs GVSK2-JP (beam aperture 5 mm, scanning optical angle ±25 deg, step response 300 μs). A laser light source with a wavelength of 650 nm (1 mW) was used. The laser source was fixed to the galvanometer mirror and mounted on a Sigma Koki stage (horizontal, TASB-652-M6, ±12.5 mm; vertical, TASB-653-M6, +7/-0 mm). A Tektronix AFG1062 function generator was used to input sinusoidal waves at 100 Hz for the galvanometer mirror. The computer was a GALLERIA ZA9C-R38 (Windows 10, Intel Core i9-10900K CPU 3.70 GHz, 32GB RAM). A 50R/50T beam splitter was used in the visible region.

A white styrene board was used for the back screen and a 3D printed slit screen (PLA, gray) was used. The distance from the camera/laser system to the slit screen was about 800 mm, and the distance to the back screen was about 1,500 mm.

B. Circle Detection Accuracy at Different Stage Position

The results of the detected circle parameters on the back screen when the stage is changed in the X direction are shown in Fig. 6, and the images at each slit screen are shown in Fig. 7. Each slit screen was replaced at each stage position, so the position of the slit screen was different each time. Then, 100 images were taken and the average of the 100 detected circle parameters was calculated. The X position of the circle center changed in response to changes in the X direction of the stage, and the Y position and radius did not change significantly.

On the other hand, the relative position of the camera and the galvanometer mirror did not change at each stage position. Therefore, the same circle parameters should be estimated for different slit screens. The proposed radial screen gave relatively constant estimation results, while the half screen showed a bias, the checker screen showed variation in the Y-center position and radius, and the stripe screen showed variation in the radius. This may be due to bias or variation in the feature points used for circle estimation. Considering manual stage adjustment and future automatic stage adjustment by actuators, it is undesirable for the circle parameter estimation to be highly dependent on the slit screen position. Thus, we have confirmed the effectiveness of the radial screen in stably estimating the circle parameters.

C. Alignment Result

The results of six alignments performed by one of the authors using the proposed calibration method are shown in Fig. 8, while saving the camera images and estimated circle parameters approximately every second during the alignment. Fig. 8a) shows the convergence of the difference of the circle parameters in the slit and back screens, and Fig. 8b) is the image after convergence. For each trial, the stages were adjusted in a different order, XYZ, XZY, YXZ, YZX, ZXY, and ZYX, respectively. If the error was still large, one of the stages was additionally adjusted. We could confirm that all the trials converged to almost similar errors. The difference between the circle parameters was less than 0.2 px, confirming that the adjustment was made with sufficient sub-pixel accuracy. The average processing time for each frame was around 24 ms, which is fast enough for real-time calibration.

Fig. 8c) shows the correspondence between the pixel coordinates of the image and the angle of the galvanometer mirror after the alignment (raster scan toward the back screen), as required in step 6 of Sec. III-D. The scanning ranges of the laser angle were -3.75 to +4.5 deg in the X direction and -3.25 to +3.5 deg in the Y direction (each in 0.25 deg increments) as the optical angle. Although it is easier to extract features by taking an image for each point projection, Fig. 8c) is a composite image of the grid points for illustration purposes.

V. Demonstration of Laser Tracking

A demonstration of high-speed high-precision laser tracking using the camera/laser scanning system calibrated by the proposed method is shown in Fig. 9. In this demonstration, near-infrared LEDs (3 mm in diameter, two pieces) were used as the tracking targets, and a visible light cut filter was attached to the camera lens so that the laser projection light could not be observed from the camera. The camera was set to 500 fps (exposure, 299 μs) for fast visual feedback. A photodiode (5 mm in diameter, photosensitive area 0.46×0.32 mm) and a visible light LED (light blue) were placed near the near-infrared LED to be tracked, and the system electrically reads (and the visible light LED glows) that the laser beam was emitted correctly. The angle voltage of the galvanometer mirror and the output voltage of the photodiode through a comparator were recorded with a data logger KEYENCE

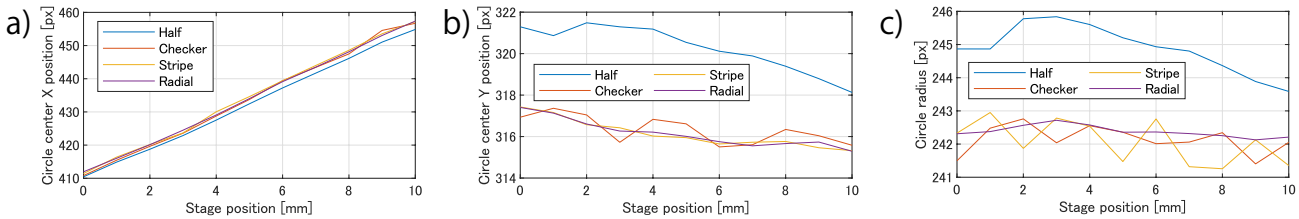

Fig. 6. Detected cricle parameters on the back screen at each stage X position; a) center X, b) center Y, and c) radius.

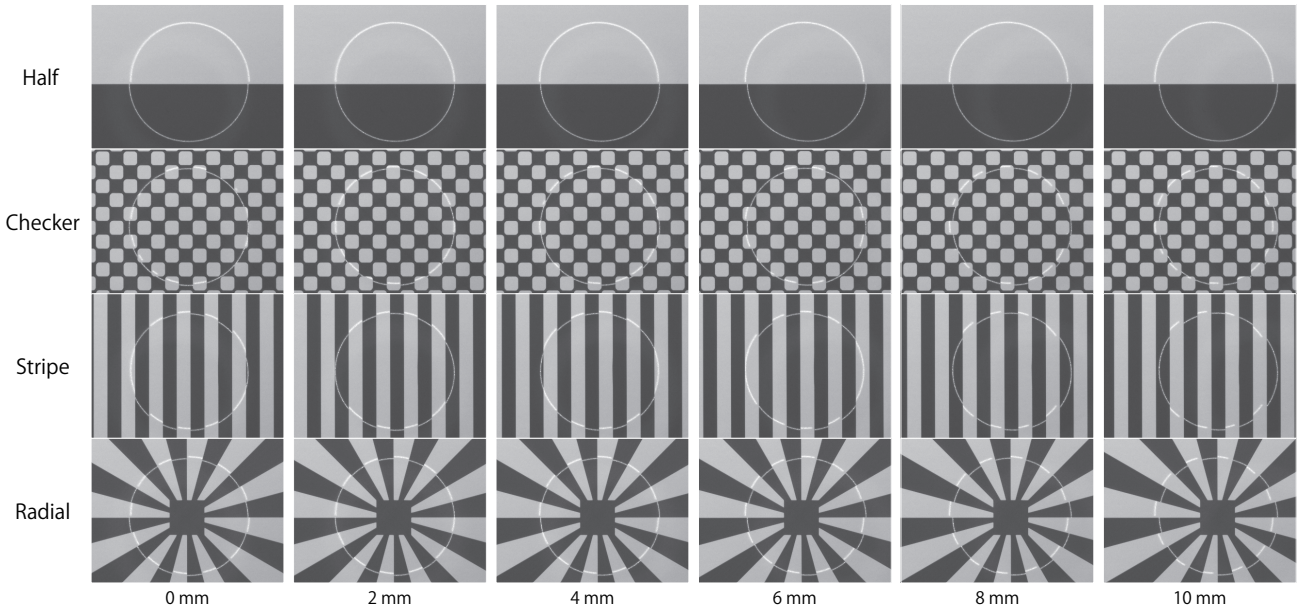

Fig. 7. Captured slit screen images with circular laser projection at each stage X position.

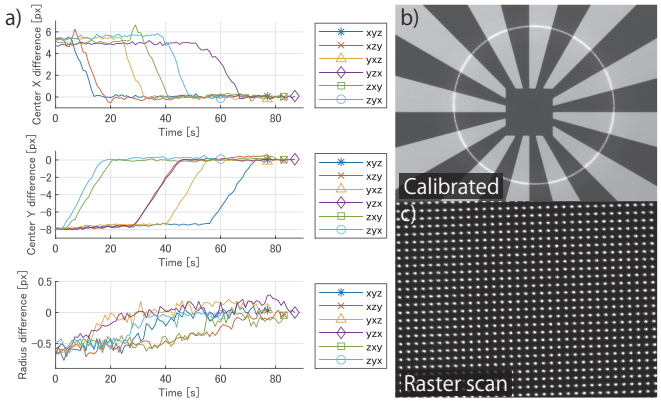

Fig. 8. Alignment results. a) convergence of circle parameter differences, b) an image after alignment, and c) raster scan for pixel-angle mapping.

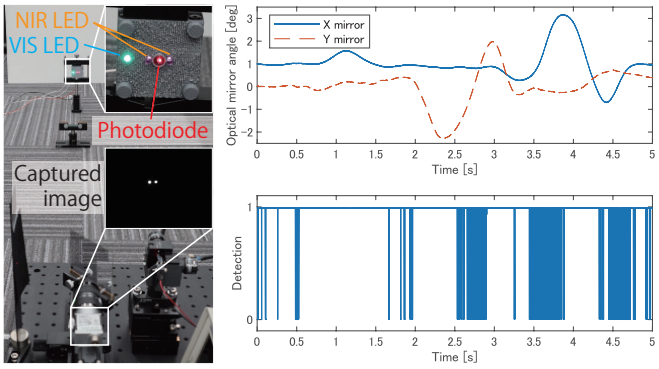

Fig. 9. Demonstration of two-dimensional laser tracking for near-infrared (NIR) lights and a photodiode.

NR-500 (every 100 μs). Such a setup is intended for actual applications such as free-space optical communications. For simplicity, we assume that lens distortion and projection distortion [21] are negligible, and use a homography matrix [14], which means a transformation between planes, for the mapping of pixels and angles by raster scan in Fig. 8c). The error between the image position transformed from the angle vector by the homography matrix and the laser point detected position was 0.76 px on average.

Fig. 9 right shows the mirror angle during tracking and the detection success or failure (1 means that enough laser light hit the photodiode). We were able to confirm that the laser light irradiated the photodiode almost continuously even when the tracking target was shaken back and forth (around 1s), up and down (around 2.5 s), and left and right (around 4s) by hand. On the other hand, photodiode chattering was also observed in some sections. During periods of fast motion, when chattering was frequent, the maximum movement

was about 0.03 deg per frame (2 ms), corresponding to 0.5 mm at about 1 m away, which is almost the same as the size of the photodiode's photosensitive area. However, there was chattering even in a nearly stationary state, and there were sections (e.g., around 4.1 s) without chattering even with fast motion. Therefore, the main cause of the bias was that the position of the center of gravity of the two near-infrared LEDs and the position of one photodiode did not exactly coincide depending on the target orientation, rather than the effect of the 500 fps laser control delay. This discrepancy in the center of gravity of the tracking target could be addressed by adjusting the laser divergence angle. The above results confirm that the optical system can be calibrated with sufficient accuracy, as the laser beam can be applied to three-dimensional motion with only two-dimensional tracking.

VI. Discussion and Conclusions

In this paper, we propose a calibration method to align the optical centers of a camera and a laser scanning system to enable laser tracking with only two-dimensional recognition for high-speed and high-precision laser tracking, which is intended for applications such as free-space communication and laser processing. We proposed a method for selecting a circle projection pattern in the laser scanning system, arranging a screen with radial slits and a back screen, and an image processing for detecting misaligned circles on the screen. Experimental results show that the radial slit is effective for stable circle parameter estimation, converging to similar adjustment results in a few trials, and a demonstration of high-speed high-precision laser tracking is also shown.

The proposed method enables quantitative visualization of optical center misalignment and precise translational alignment. The limitation of the proposed method is the range where the screen can be installed. It is difficult to install a large screen in a distant place for long-distance applications such as the free-space communication. On the other hand, for sufficiently distant laser projection, small misalignments of the optical center can be ignored, and sufficient calibration performance can be expected for screens within the range of possible installation.

In the future, we will attempt to develop a method that enables higher accuracy and wider range of calibration corresponding to lens distortion and laser projection distortion. We will also evaluate the effects of screen placement and projection radius, assess the efficiency of the calibration procedure, and realize a high-speed high-precision laser tracking system for distant motion and various applications for irregular motion.

References

[1] Yagiz Kaymak, Roberto Rojas-Cessa, Jianghua Feng, Nirwan Ansari, MengChu Zhou, and Tairan Zhang. A survey on acquisition, tracking, and pointing mechanisms for mobile free-space optical communications. *IEEE Communications Surveys & Tutorials*, 20(2):1104–1123, 2018.

[2] Alberto Carrasco-Casado, Ricardo Vergaz, José M Sánchez-Pena, Eva Otón, Morten A Geday, and José M Otén. Low-impact air-to-ground free-space optical communication system design and first results. In *2011 International Conference on Space Optical Systems and Applications (ICSOS)*, pages 109–112. IEEE, 2011.

[3] Mangirdas Malinauskas, Albertas Žukauskas, Satoshi Hasegawa, Yoshio Hayasaki, Vygantas Mizeikis, Ričardas Buividas, and Saulius Juodkazis. Ultrafast laser processing of materials: from science to industry. *Light: Science & Applications*, 5(8):e16133, 2016.

[4] Nikita Levichev, Gonçalo Costa Rodrigues, Vitalii Vorkov, and Joost R Duflou. Coaxial camera-based monitoring of fiber laser cutting of thick plates. *Optics & Laser Technology*, 136:106743, 2021.

[5] Ho Yeung, Brandon M Lane, MA Donmez, and S Moylan. In-situ calibration of laser/galvo scanning system using dimensional reference artefacts. *CIRP Annals*, 69(1):441–444, 2020.

[6] Seppe Sels, Boris Bogaerts, Steve Vanlanduit, and Rudi Penne. Extrinsic calibration of a laser galvanometric setup and a range camera. *Sensors*, 18(5):1478, 2018.

[7] Toshiyuki Amano. Projection center calibration for a co-located projector camera system. In *Proceedings of the IEEE Conference on Computer Vision and Pattern Recognition Workshops*, pages 443–448, 2014.

[8] Yuri Mikawa, Tomohiro Sueishi, Tomohiko Hayakawa, and Masatoshi Ishikawa. Laser-based drawing method for posture-free objects by photochromic active marking with high-speed coaxial gaze control. In *SPIE Photonics West, Laser 3D Manufacturing VII*, volume 11271, pages 1–8, 2020.

[9] Hiromasa Oku, Alvaro Cassinelli, Masahiko Yasui, and Masatoshi Ishikawa. Information presentation device. US Patent, US10142601B2, 2013.

[10] Kosuke Mori, Masanori Terada, Kazuki Nakamura, Ryoji Murakami, Kunitake Kaneko, Fumio Teraoka, Daisuke Yamaguchi, and Shinichiro Haruyama. Fast handover mechanism for high data rate ground-to-train free-space optical communication system. In *2014 IEEE Globecom Workshops (GC Wkshps)*, pages 499–504, 2014.

[11] Zewei Liu, Dongming Lu, Weixian Qian, Guohua Gu, Kan Ren, Jun Zhang, and Xiaofang Kong. Calibration of a single-point laser range finder and a camera. *Optical and Quantum Electronics*, 50:447, 2018.

[12] Kohei Okumura, Keiko Yokoyama, Hiromasa Oku, and Masatoshi Ishikawa. 1 ms Auto Pan-Tilt–video shooting technology for objects in motion based on Saccade Mirror with background subtraction. *Advanced Robotics*, 29(7):457–468, 2015.

[13] Tomohiro Sueishi, Hiromasa Oku, and Masatoshi Ishikawa. Lumipen 2: Dynamic projection mapping with mirror-based robust high-speed tracking against illumination changes. *Presence*, 25(4):299–321, 2016.

[14] Kenta Yamamoto, Daisuke Iwai, Ikuho Tani, and Kosuke Sato. A monocular projector-camera system using modular architecture. *IEEE Transactions on Visualization and Computer Graphics*, 29(12):5586–5592, 2022.

[15] Shujun Huang, Lili Xie, Zhangying Wang, Zonghua Zhang, Feng Gao, and Xiangqian Jiang. Accurate projector calibration method by using an optical coaxial camera. *Applied Optics*, 54(4):789–795, 2015.

[16] Veljko Milanovic, Gabriel A Matus, and Daniel T McCormick. Gimbal-less monolithic silicon actuators for tip-tilt-piston micromirror applications. *IEEE Journal of Selected Topics in Quantum Electronics*, 10(3):462–471, 2004.

[17] Tomohiro Sueishi, Ryota Nishizono, and Masatoshi Ishikawa. Emndash: A robust high-speed spatial tracking system using a vector-graphics laser display with m-sequence dashed markers. *Journal of Robotics and Mechatronics*, 34(5):1085–1095, 2022.

[18] Osama Halabi and Norishige Chiba. Efficient vector-oriented graphic drawing method for laser-scanned display. *Displays*, 30(3):97–106, 2009.

[19] Nikolai Chernov. *Circular and linear regression: Fitting circles and lines by least squares*. CRC Press, 2010.

[20] Zygmunt L Szpak, Wojciech Chojnacki, and Anton Van Den Hengel. A comparison of ellipse fitting methods and implications for multiple-view geometry estimation. In *2012 International Conference on Digital Image Computing Techniques and Applications (DICTA)*, pages 1–8. IEEE, 2012.

[21] Peter E Verboven. Distortion correction formulas for pre-objective dual galvanometer laser scanning. *Applied Optics*, 27(20):4172–4173, 1988.

[22] Tongjie Y Zhang and Ching Y. Suen. A fast parallel algorithm for thinning digital patterns. *Communications of the ACM*, 27(3):236–239, 1984.

[23] Tomohiro Sueishi and Masatoshi Ishikawa. Ellipses ring marker for high-speed finger tracking. In *Proceedings of the 27th ACM Symposium on Virtual Reality Software and Technology*, pages 1–5, 2021.